Published in final edited form as:

Cell Rep. 2016 August 23; 16(8): 2142–2155. doi:10.1016/j.celrep.2016.07.055.

Phosphorylation-Induced Motor Shedding is Required at Mitosis for Proper Distribution and Passive Inheritance of Mitochondria

Jarom Yan-Ming Chung[1,2], **Judith Arunodhaya Steen**[1], and **Thomas Lewis Schwarz**[1,2,*]

[1]The F.M. Kirby Neurobiology Center, Boston Children's Hospital, Boston MA 02115. USA

[2]Department of Neurobiology, Harvard Medical School, Boston MA 02115. USA

Abstract

While interphase mitochondria associate with microtubules, mitotic mitochondria dissociate from spindle microtubules and localize in the cell periphery. Here, we show that this redistribution is not mediated by mitochondrial active transport or tethering to the cytoskeleton. Instead, kinesin and dynein, that link mitochondria to microtubules, are shed from the mitochondrial surface. Shedding is driven by phosphorylation of mitochondrial and cytoplasmic targets by CDK1 and Aurora A. Forced recruitment of motor proteins to mitotic mitochondria to override this shedding prevents their proper symmetrical distribution and disrupts the balanced inheritance of mitochondria to daughter cells. Moreover, when mitochondria with bound dynein bind to the mitotic spindle, they arrest cell cycle progression and produce binucleate cells. Thus, our results show that the regulated release of motor proteins from the mitochondrial surface is a critical mitotic event.

Graphical Abstract

[*]Correspondence: thomas.schwarz@childrens.harvard.edu.

Author Contribution

T.L.S. and J.A.S. conceived and supervised the study. T.L.S. and J.Y.C. designed experiments and wrote the manuscript. J.Y.C. performed the experiments and generated the figures and tables. All authors discussed the data and commented on the manuscript prior to submission.

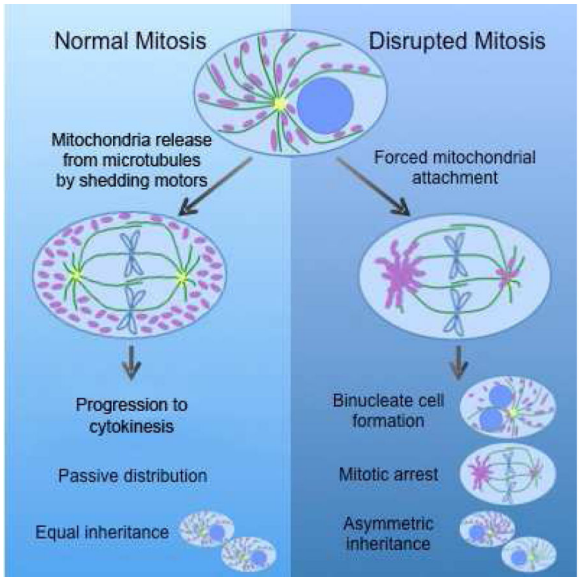

Introduction

Preceding cell division, the cell orchestrates processes that ensure two functional daughter cells. While many investigations focus on chromosomal duplication and segregation, mitochondria contain their own DNA and therefore cannot be formed de novo. Thus, their proper inheritance by daughter cells must also be ensured. To this end, mitochondria increase their number early in mitosis through biogenesis and fission (Kashatus et al., 2011; Martinez-Diez et al., 2006). Although much is known about mitochondrial inheritance in yeast, where it depends on movement of healthy mitochondria along actin filaments into the daughter cell (Westermann, 2014), the mechanism in metazoans remains unknown (Mishra and Chan, 2014).

Two modes of organelle inheritance are hypothesized: active and passive. Active segregation in metazoans is carried out through attachment to microtubules primarily, a prime example being chromosomal inheritance. For passive segregation, organelles are not associated with the cytoskeleton and a simple increase in their abundance is thought to allow for stochastic and balanced inheritance into daughter cells (Symens et al., 2012). Mitochondria are thought to undergo passive inheritance, although it is unclear how it comes about. As the cell enters mitosis, mitochondria fragment through a combination of increased DRP1 and degradation of the mitochondrial fusion factor MFN1 by MARCH-V (Kashatus et al., 2011; Park and Cho, 2012). However, for passive inheritance to occur, mitochondria must also release from cytoskeletal anchors and distribute evenly throughout the cytoplasm, which fragmentation alone does not guarantee (Mishra and Chan, 2014). Conflicting reports have implicated microtubules and actin as active drivers of mitochondrial inheritance, but it remains unknown how these elements would position mitochondria during cell division (Lawrence and Mandato, 2013c; Lee et al., 2007; Rohn et al., 2014).

Mitochondria move along microtubules through a motor adaptor complex consisting of an atypical rho-GTPase Miro (RhoT1/2) on the outer mitochondrial membrane, the motor

adaptor Milton (Trak1/2, OIP106/98), kinesin heavy chain (KHC, KIF5), and dynein/dynactin complexes. Both Miro and Milton are essential for attaching the motor proteins to the mitochondrial surface and hence for mitochondrial movement (Fransson et al., 2006; Glater et al., 2006; Guo et al., 2005; Stowers et al., 2002; van Spronsen et al., 2013). Additionally, mitochondria are known to attach to actin and the ER (de Brito and Scorrano, 2008; Pathak et al., 2010). These attachments contribute to proper mitochondrial distribution and function during interphase.

To date, it is still unclear how mitochondrial distribution and cytoskeletal association affect inheritance by daughter cells (Mishra and Chan, 2014). While examining mitotic cells, we observed a marked shift in the relationship of mitochondria to the microtubule network. We tested likely mechanisms for active control of mitochondrial distribution, including peripheral tethers. We found evidence instead for passive mitochondrial positioning and inheritance. We therefore examined the regulation of the motor adaptor complex and demonstrated that release of motors from the complex is required for proper mitochondrial inheritance and the fidelity of cell division.

Results

Mitochondria are released from microtubules during cell division and remain peripheral to the mitotic spindle

We have examined by confocal microscopy the relationship of mitochondria to the microtubule network in HeLa cells that were synchronized with a double thymidine block (Figure 1A). During interphase, the mitochondria are overwhelmingly associated with microtubules, as expected from their known dynamic movement along these tracks (Ball and Singer, 1982). In contrast, mitochondria do not colocalize with the mitotic spindle, a phenomenon most apparent in an optical section through the center of the cell. In fixed images and live imaging, mitochondria are released from microtubules once the cell enters mitosis and indeed appear to be repelled from the space occupied by the spindle (Figure 1A). When viewed in a 3D reconstruction, mitotic cells have a central core of the spindle and chromosomes, which is surrounded by a peripheral mitochondrial zone. Where mitochondria are close to astral microtubules, the mitochondria are not oriented adjacent or parallel to these microtubules, as they are in interphase, but rather appear to ignore the microtubules in their vicinity. We calculated percent overlap between mitochondria and tubulin as a fraction of the total mitochondrial signal during the cell cycle and found that overlap significantly decreases at the onset of mitosis (Figure 1B). The residual overlap probably represents the incidental overlap of astral microtubules and peripheral mitochondria. The same phenomenon was observed in HEK293T cells, COS cells, and primary cultures of rat embryonic fibroblasts (Figure S1A). Mitochondria thus appear to detach from microtubules during cell division.

To characterize the timing of mitochondrial detachment from microtubules, we analyzed both live and fixed cells during mitosis (Figure 1D, S1B, Video S1). We graphed the signal distribution of DNA, tubulin, and mitochondria relative to the center of the DNA signal using the “Radial Profile” ImageJ plugin (Baggethun, 2009) (Figure 1C,D). During interphase, tubulin and mitochondria have similar, overlapping distribution patterns, which

persists as the cell enters prophase. When the cell enters prometaphase, however, the microtubule network depolymerizes and shifts towards the center of the cell to form the mitotic spindle (Video S1,S2). In contrast, the mitochondria remained in place without any consistent translocation that would indicate microtubule-based movement towards the periphery. The mitotic cell, however, became rounded and in consequence the cell perimeter moved closer to where the mitochondrial already were present. Thus, the largely stationary mitochondria appeared more peripheral while the spindle formed in the mitochondria-free zone that was formerly the nucleus. Mitochondria remained dissociated from microtubules until reattachment during telophase (Figure 1B,D, Video S3). Overall, we concluded that the peripheral localization of mitochondria during mitosis was caused primarily by their release from the reorganizing microtubules and rather than active transport.

Mitochondria are not tethered away from the spindle

A potential mechanism for mitochondrial redistribution during mitosis would be tethering to a cytoskeletal element or membrane distant from the spindle. To further examine this possibility, we tested the possible role of two known associations of mitochondria, actin and the endoplasmic reticulum (ER). Mitochondria interact with actin microfilaments (Pathak et al., 2010), and it has been suggested that their peripheral localization arises from association with the actin network (Lee et al., 2007). We synchronized HeLa cells and treated with the actin depolymerizing agent Latrunculin A or the vehicle DMSO alone for 10 minutes before fixation. In control conditions, the actin-rich region and the mitochondrial zone were quite distinct with the actin shell peripheral to the mitochondria (Figure 2A). Latrunculin treatment abolished the actin network but the mitochondrial distribution was not altered; mitochondria did not re-associate with the spindle during Latrunculin treatment (Figure 2B). We concluded that actin had not tethered mitochondria away from the spindle.

Mitochondria form contacts with the ER (de Brito and Scorrano, 2008) and, like mitochondria, the ER attaches to microtubules during interphase. It is released from microtubules during mitosis via the phosphorylation of STIM1 (Smyth et al., 2012) and, once in the periphery, could conceivably hold associated mitochondria there as well. We therefore used a phosphoresistant mutation of STIM1 that mislocalizes ER onto the spindle (Figure S2E) (Smyth et al., 2012). We transiently expressed STIM1 wild type (WT) or the mutant version (10A) in HeLa cells, followed by synchronization and imaging (Figure 2C). Although the STIM1 10A construct forced ER onto the spindle and made the spindle slightly wider, mitochondria did not follow the ER onto the spindle (Figure 2D). The localization of the ER does not determine the position of the mitochondria.

To ask more generally if mitochondria were anchored in the periphery or just sterically prevented by the spindle from invading the central area, we used nocodazole to depolymerize microtubules (Figure 2E, Video S4). As the spindle depolymerized, mitochondria immediately moved into that space and were only excluded from the area occupied by the dense chromosomes (Figure S2F). Taken together, these data suggest that mitochondria are not tethered in the periphery and the microtubule rich spindle sterically occludes mitochondria.

Motor proteins are released from mitochondria during cell division

The switch from an intimate relationship of mitochondria and microtubules in interphase to their abrupt divorce during mitosis suggested a change in the proteins that underlie the relationship. The clearest connection between them is that mediated by the motor proteins dynein, dynactin, and kinesin (Figure 3A). We therefore asked if the motor proteins were degraded or lost their association with mitochondria. HeLa cells were synchronized using a double thymidine block for interphase and were synchronized for mitosis with a single thymidine block followed by addition of nocodazole. Cells were lysed and analyzed by western blot (Figure 3B). Because dynein and dynactin are composed of many components, we measured dynein intermediate chain (DIC) to assay dynein and p150 for dynactin. Levels of DIC, conventional kinesin-1 (KHC), p150, and the adaptor proteins Milton, and Miro did not significantly change between interphase and mitosis ($p > 0.1$) (Figure 3C). DIC and p150 both exhibited a band shift, previously known to be due to phosphorylations. Milton also exhibited a large band shift.

To determine if the complex remained on mitochondria, we isolated mitochondria from interphase and mitotic cells. DIC, p150, and KHC levels on mitochondria decreased during mitosis (Figure 3B,D). Miro levels remained unchanged ($p=0.16$), but Milton was more abundant ($p=0.019$). Cyclin B also associates with mitochondria, as has been previously reported (Kashatus et al., 2011). The selective loss of the motor proteins from mitotic mitochondria was verified with S-trityl-L-cysteine instead of nocodazole to synchronize cells (Figure S3E). Myc-hMilton1 was expressed with HA-Miro1 and motors in HeLa cells for analysis by immunocytochemistry at interphase and metaphase. Miro and Milton colocalized with the mitochondrial marker TOM20 both during interphase and mitosis and did not overlap with the spindle (Figure S3D). As previously observed (Glater et al., 2006), overexpressed KHC colocalized with Milton and mitochondria during interphase and induced peripheral aggregates of mitochondria, consistent with excessive transport to (+) ends. During mitosis, KHC was diffuse throughout the cytoplasm and enriched on the spindle, consistent with the biochemical observation of kinesin loss from mitochondria (Figure S3A). Although DIC was not as predominantly mitochondrial as KHC, DIC overexpression caused perinuclear clustering of mitochondria during interphase, consistent with excess traffic to (−) ends. During mitosis, DIC was diffuse in the cytosol but also noticeably present on the spindle (Figure S3B). p150 was diffusely cytoplasmic during interphase, but highly enriched on the mitotic spindle during cell division (Figure S3C). The biochemical and immunocytochemical characterization (Figure 3B, S3) pointed to a motor-shedding hypothesis in which Miro and Milton remain on mitochondria but dynein, dynactin, and kinesin detach from these adaptor proteins during cell division.

Motor release is induced by phosphorylation

To probe the mechanism of motor shedding, we developed an *in vitro* motor shedding assay by isolating mitochondrial and cytosolic fractions from interphase and mitotic cells. Mitochondria from each phase were mixed with interphase or mitotic cytosol. After a two-hour incubation, mitochondria were isolated and analyzed by western blot (Figure 3E). Interphase mitochondria, which originally had high levels of both DIC and KHC, lost these motors when incubated with mitotic but not interphase cytosol (Figure 3E,F,G). We did not,

however, observe the large phosphorylation-dependent band shift in Milton or DIC, indicating that the *in vitro* incubation, though sufficient to cause motor release, did not fully recapitulate all mitotic events. In a reciprocal experiment, DIC and KHC reattached onto mitotic mitochondria following incubation with interphase but not mitotic cytosol (Figure 3H). We concluded that mitotic cytosolic factors were sufficient to release motors from mitochondria, and interphase cytosolic factors were able to reattach motors.

Because phosphorylation governs much of mitosis, we hypothesized that phosphorylation triggered motor shedding. Calf intestinal phosphatase (CIP) was used to dephosphorylate mitochondrial or cytosolic fractions isolated from mitotic cells (Figure 3I). When untreated mitotic mitochondria were incubated with untreated mitotic cytosol, motors, as expected, did not significantly reattach to mitochondria (Figure 3J,K,L). Combining CIP-treated mitochondria with untreated cytosol caused a slight increase in bound DIC and KHC ($p=0.059$, $p=0.207$). When CIP-treated cytosol was added to untreated mitochondria, KHC reattached significantly ($p=0.018$), and KHC attachment increased similarly after CIP treatment of both fractions. DIC levels increased only slightly after CIP treatment of mitochondria ($p=0.063$) but DIC increased robustly when both mitochondria and cytosol were treated ($p=0.033$). We concluded that motor shedding is dependent on phosphorylation and dynein detachment is driven by changes to both cytosolic and mitochondrial proteins while KHC association with mitochondria is primarily dependent on cytosolic phosphorylations.

CDK1 induces dynein release, and Aurora A induces kinesin release

We subsequently asked which kinases induce motor release. Cyclin-dependent kinase 1 (CDK1) and its cofactor cyclin B are the primary drivers of mitosis; we therefore tested whether CDK1 could induce motor shedding when applied to interphase mitochondria. Isolated interphase mitochondria were treated with active CDK1 for an hour and then washed (Figure 4A). DIC levels on the CDK1-treated mitochondria decreased compared to the untreated (Figure 4B,C). In contrast, there wasn't a significant change in KHC bound. We tested other downstream kinases and found that Aurora A was sufficient to induce KHC but not dynein shedding (Figure 4B–D). Shedding was not synergistically enhanced by combining CDK1 and Aurora A. Thus the two motors were released by distinct kinases.

To test the necessity of CDK1 and Aurora A in motor shedding, we treated synchronized mitotic cells with a CDK1 inhibitor (RO-3306), an Aurora A inhibitor (ZM 447439), or the vehicle control (Figure 4E). As expected CDK1 inhibition, which is upstream of Auora A, reattached dynein and kinesin back onto the mitochondrial surface. Aurora A inhibition, however, did not increase DIC or kinesin attachment (Figure 4F,G). Taken together with our in vitro data, we concluded that Aurora A was sufficient to release kinesin but other kinases likely cause kinesin shedding as well. To test the sufficiency of Auora A for kinesin release in cells, we expressed constitutively active (T288D) and kinase dead (K162R) constructs in HEK293T cells synchronized in interphase (Figure 4H). The constitutively active Aurora A was sufficient to detach kinesin but not DIC (Figure 4I). In addition, active Aurora A phosphorylated Milton, which also occurred in reactions *in vitro* (Figure 4B,I).

Preventing Milton or kinesin phosphorylations is not sufficient to prevent motor release

We took a candidate approach to identifying the regulatory phosphorylations. Milton was a strong candidate because of the large band shift seen during mitosis and CIP treatment eliminated the shift (Figure S4A). By mass spectroscopy of synchronized HeLa cells, we found 28 Milton phosphorylation sites (Figure S4B) and mutated all of them in hMilton1 to alanines to create a phosphoresistant mutant (Milton 28A). Although this produced a functional Milton that localized to mitochondria and bound motor proteins, the 28A mutant was unable to prevent motor release or change the distribution of mitochondria during mitosis (Figure S4C,D). Likewise, mitochondria containing the 28A mutant behaved in vitro like those with wildtype Milton; DIC reattached equivalently to both when CIP-treated mitotic cytosol was added (Figure S4E,F).

In a phosphoproteomics study of the cell cycle, kinesin, dynein, and dynactin proteins were found to be phosphorylated during mitosis (Olsen et al., 2010). Because kinesin detachment was driven by phosphorylation in the cytosolic fraction (Figure 3F), we mutated two previously reported phosphorylation sites (S917, S938) on kinesin heavy chain that fall near the Milton-binding domain (residues 810–891) (Glater et al., 2006; Olsen et al., 2010). Upon expression of our phosphoresistant kinesin, we saw neither increased kinesin attachment during mitosis nor a change in mitochondrial distribution (Figure S4G,H). We concluded that preventing phosphorylation at those sites was not sufficient to prevent motor shedding.

Motor attachment mislocalizes mitotic mitochondria

Since we were unable to determine the exact targets for motor release, we used two strategies to artificially attach motors during mitosis and thereby determine the cellular consequences of overriding motor shedding. One approach used a temporally-controlled attachment using the heterodimerizing drug rapalog (A/C Heterodimerizer, Clontech), which links proteins containing the FKBP and FRB domains (Figure S5A). The second strategy used a motor fused to a mitochondrially targeted domain (Figure S5B). To induce dynein attachment with rapalog, we transfected HeLa cells with an FKBP domain targeted to the mitochondrial surface (TOM20-mCherry-FKBP) and with an FRB domain attached to Bicaudal D2 (HA-BICD2-FRB), a known adaptor for dynein and dynactin (Hoogenraad et al., 2003). During interphase, rapalog addition caused the mitochondrial network to collapse onto the microtubule-organizing center (Figure S5C). Cells were synchronized into mitosis and rapalog or ethanol (the vehicle control) was added ten minutes prior to fixation (Figure 5A). After rapalog addition, mitochondria were no longer in the periphery and instead localized onto the spindle (Figure 5B); mitochondria and tubulin consequently overlapped significantly more than in control cells (Figure 5C, Video S5). When BICD was linked directly to the outer mitochondrial membrane, mitochondria also localized to the spindle apparatus (Figure S5D). Thus dynein recruitment to the mitochondrial surface results in reattachment of the mitochondria to microtubules and their mislocalization onto the mitotic spindle. In addition to illustrating the necessity of dynein-shedding for proper mitochondrial localization, it also confirms that spindle microtubules are still able to bind motors.

We tested kinesin attachment with similar protocols, but our constitutive kinesin attachment construct compromised the integrity of the mitochondria and was therefore not used (data

not shown). Instead, we transfected cells with a KIF5B motor domain-FRB domain fusion (HA-KIF5B MD-FRB) along with the TOM20-mCherry-FKBP construct. During interphase, the addition of rapalog drove mitochondria to the periphery (Figure S5C), as expected for the (+) end directed motor. Upon rapalog addition during metaphase, we also observed that the mitochondria were pushed towards the cell periphery (Figure 4D,E). As a result, rapalog significantly reduced mitochondria-microtubule overlap (Figure 4F). During mitosis, microtubule plus ends are found both towards the center of the spindle (kinetochore/polar microtubules) and towards the periphery (astral microtubules). Out of 90 mitotic cells analyzed only 5 cells had any mitochondria attached to the spindle, and this only occurred when we treated cells with rapalog during prometaphase (Figure 6A). The proximity of mitochondria to astral rather than spindle microtubules likely biases them to peripheral movement.

Motor attachment can cause asymmetric mitochondrial distribution and inheritance

Besides localizing mitochondria onto the spindle, the reattachment of motors to mitochondria produced additional phenotypes. The symmetry of mitochondrial distribution at metaphase was disrupted when either dynein or kinesin were reattached to mitochondria, but the asymmetries differed in their severity (Figure 5A). With dynein attachment, the extent of asymmetry depended on the timing of rapalog addition. Rapalog-induced dynein attachment to mitochondria during G2 or prometaphase induced severe asymmetry whereas dynein attachment during metaphase did not (Figure 5B). Mitochondria also were asymmetrically distributed upon rapalog-induced kinesin reattachment, but this effect was independent of when rapalog was added (Figure 5C).

To determine if the induced-asymmetries during metaphase would persist throughout mitosis, we allowed rapalog-treated and control cells to proceed into telophase prior to fixation (Figure 5D). Overall there was a lesser degree of asymmetry compared to the high asymmetry observed when either dynein ($p = 0.13$) or kinesin ($p = 0.04$) were recruited to mitochondria during metaphase, but there were still cells that inherited mitochondria asymmetrically. We performed live imaging of cells expressing HA-BICD2-FRB or HA-KIF5B MD-FRB and watched cells with high asymmetry during metaphase as they proceeded through mitosis. Asymmetry that occurred in metaphase persisted during telophase albeit to a lesser degree (Video S6,S7). Since the asymmetry diminished during telophase, there may be compensatory mechanisms that act to normalize the distribution. Some of these mechanisms may involve Myosin XIX, Kif5B, or a CENP-F/Miro/EB1 association, as reported by others in the literature (Kanfer et al., 2015; Lawrence and Mandato, 2013a; Rohn et al., 2014).

Mitochondrial localization to the spindle interferes with progression through mitosis

To measure the effect of mitochondrial attachment on mitosis, we synchronized cells expressing the mito-FKBP construct and either BICD-FRB or KIF5B–FRB. Upon release from thymidine block cells were treated with rapalog or the vehicle control. Beginning 8 hours after release, when the maximum number of cells were mitotic, samples were taken at 30 minute intervals and fixed. The percentage of mitotic cells was calculated for each time point. In controls, 30% of cells were mitotic 8 hours after release from thymidine, and this

percentage gradually decreased over the hours to less than 10%. Most BICD-FRB transfected cells treated with rapalog, however, did not undergo cytokinesis; the percent in mitosis after 11 hours remained at 25% (Figure 7A). In contrast, control and rapalog treated cells transfected with KIF5B–FRB exited mitosis equivalently (Figure 7B).

To assess the impact of mitochondrial redistribution onto the spindle, we counted binucleate cells as a measure for cytokinesis failure. HeLa cells transfected with BICD-FRB and mito-FKBP were synchronized and treated with rapalog or the vehicle control during G2. Cells were allowed to proceed through one cell division before fixation. Binucleate cells were rare in control conditions (3% of cells) but increased to greater than 50% with rapalog treatment (Figure 7C,D). Expression of BICD that was constitutively targeted to mitochondria also significantly increased binucleate cells although to a lesser extent (Figure S7A,B). Recruitment of KIF5B-FRB to mitochondria with rapalog did not increase binucleate cells. Thus, while redistribution of mitochondria to the cell's periphery with kinesin recruitment may cause asymmetry, it neither delayed mitotic progression nor blocked cytokinesis to create binucleate cells. In contrast, redistribution of mitochondria onto the spindle strongly interfered with mitotic progression and resulted in a high percentage of binucleate cells.

The binucleate cells might have arisen as a consequence of mitochondrial attachment or by sequestering endogenous dynein away from other mitotic functions. Some disruption of normal dynein functions in these cells may have been indicated by a change of spindle angle (Figure S7D) (Raaijmakers et al., 2013). We therefore used a peroxisome targeted FKBP domain (PEX-mRFP-FKBP) to sequester dynein onto peroxisomes and compared the consequences to those of mitochondrial recruitment. Recruitment of dynein mislocalized peroxisomes onto the spindle (Figure S7C) but did not significantly increase binucleate cells (Figure 7C,D). Although both peroxisomes and mitochondria sequestered endogenous dynein, only mitochondrial attachment prevented correct cytokinesis, suggesting that it was not dynein sequestration per se, but rather the steric consequences of mitochondria on the spindle that was deleterious. To further test this hypothesis, we used STIM1 10A to prevent ER release from spindle microtubules. Cells were transfected with either STIM1 wild type (WT) or the phosphoresistant 10A mutant and after 48 hours synchronized as before and fixed to analyze the percentage of binucleate cells. Although this chronic change in ER behavior differs from the acute changes to organelles induced by rapalog addition, binucleate cells increased significantly in the STIM1 10A expressing cells (Figure 7C,D). Thus, the presence of large organelles on the spindle, whether mitochondria or the ER, will interfere with mitosis and cause binucleate cells.

Discussion

We have determined that (1) mitochondria are released from microtubules during cell division; (2) mitochondria passively remain in the periphery by dissociation from microtubules rather than by active transport into the periphery or anchoring; (3) this dissociation is achieved by shedding dynein and kinesin motors from the Miro/Milton motor adaptor complex through CDK1 and Aurora A kinase phosphorylation of mitochondrial and cytosolic substrates; (4) engineered dynein attachment during mitosis forces mitochondria onto the spindle apparatus, whereas kinesin attachment pushes mitochondria further into the

periphery; (5) motor shedding is crucial for correct mitochondrial distribution during metaphase and balanced mitochondrial inheritance by daughter cells; and (6) if mitochondria are present on mitotic microtubules, progression through the cell cycle is arrested and binucleate cells arise.

Prior to this study, there were conflicting results about mitochondrial distribution and attachment to cytoskeletal elements like tubulin and actin (Lawrence and Mandato, 2013c; Lee et al., 2007; Martinez-Diez et al., 2006; Mishra and Chan, 2014; Rohn et al., 2014). In our study, we show that mitochondria-microtubule interactions are disrupted as the cell enters mitosis (Figure 1). Some discrepancies may have arisen because mitochondria surrounding the microtubulerich core appear to overlap by epifluorescent microscopy. Further, we found that the peripheral mitochondrial distribution can be explained as a passive consequence of release from microtubules, with no evidence for active transport away from the spindle or tethering to peripheral actin or ER (Figure 2, Video S1,S2). We therefore focused on the mechanisms behind release from microtubules although other associations of mitochondria may also be disrupted and then reform during telophase and contribute to mitochondrial inheritance.

Release of kinesin and dynein from Miro and Milton is induced by phosphorylation. Although a previous study observed that dynein was dissociated from mitochondria (Lee et al., 2007), the state of the other components of the motor adaptor complex (kinesin, Miro, Milton) and the physiological significance of dynein dissociation was not known. We found that Miro and Milton are maintained on the mitochondrial surface when the motors are shed (Figure 3). By forcing motors onto mitochondria, we showed that motor release was necessary for disassociation from microtubules (Figure 4). Even at metaphase, when mitochondria are furthest from the spindle, dynein reattachment forced them onto it (Video S5).

Phosphorylation by CDK1 accounted for dynein release and Aurora A for kinesin. Both mitochondrial and cytoplasmic protein phosphorylations mediated dynein release, whereas phosphorylations in the cytoplasmic fractions mediated kinesin release. Dynein release from membranous structures may be a general feature of cell division. In Xenopus membrane preparations, dynein and dynactin components were lower in mitotic than in interphase membrane fractions. In motility assays, mitotic membrane fractions had decreased microtubule-based transport, which was restored by incubation with interphase cytoplasm. Likewise incubation of membranes with CDK1 resulted in decrease of dynein attachment in Xenopus extracts (Allan and Vale, 1991; Dell et al., 2000; Niclas et al., 1996).

Our data strongly indicated the presence of redundant phosphorylation targets. For instance, dynein reattachment only occurred when both cytosolic and mitochondrial phosphorylations were removed by phosphatase. Furthermore, Aurora A was sufficient but not necessary to induce kinesin release, and a redundant kinases can likely cause kinesin shedding as well. The degree of redundant mechanisms for motor shedding likely explains why reversing the extensive phosphorylation of Milton was nonetheless insufficient to reverse the dissociation of the motors. Interestingly, CDK1 and Aurora A phosphorylation increase mitochondrial

fission, as well (Kashatus et al., 2011), a process intimately related to mitochondrial movement.

The redundant mechanisms for motor shedding may reflect its importance to mitosis. Overriding the shedding induced asymmetric mitochondrial inheritance, mitotic delay, and formation of binucleate cells. The degree of asymmetric mitochondrial distribution at metaphase depended on the timing of dynein reattachment (Figure 6). A likely explanation lies in the process of centrosome migration (Figure S6C). If rapalog drives mitochondrial collapse around the microtubule-organizing center prior to centrosome migration during G2 or prometaphase, most mitochondria will remain associated with the extensive microtubule array of the stationary centrosome, and few will follow the migrating centrosome to the opposite pole, thereby producing an asymmetry. Only minor asymmetry occurs upon reattachment of dynein during metaphase, when the two centrosomes have separated and microtubules are symmetric.

The requirement for motor shedding for symmetric inheritance opens the question of whether its regulation mediates asymmetric inheritance of mitochondria in special circumstances. During asymmetric stem cell divisions, the daughter that retains a stem cell nature inherits young mitochondria whereas older mitochondria are inherited by the more differentiated cell (Katajisto et al., 2015). The mechanism behind this phenomenon is still unknown, but the passive nature of mitochondrial inheritance described in the present study implies that an age-dependent mitochondrial asymmetry established in interphase stem cells could passively bias their segregation in mitosis. Alternatively, retention of dynein on a subpopulation of mitochondria early in mitosis would cause them to be retained by the stationary centrosome and share its subsequent destiny in the stem cell.

We found that the asymmetry of metaphase mitochondrial distribution could persist into cytokinesis and cause asymmetric mitochondrial inheritance, albeit somewhat attenuated (Figure 6). This suggests compensatory mechanisms occur to correct for proper inheritance. Indeed, studies have found that cytoskeletal attachments play important roles during later stages of mitosis. Myosin XIX has been found to affect mitochondrial inheritance (Rohn et al., 2014). Furthermore, EB1/CENP-F/Miro and KHC/Miro have been found to move mitochondria towards the cleavage furrow during telophase (Kanfer et al., 2015; Lawrence and Mandato, 2013a; Lawrence et al., 2016). These attachments, acting later in mitosis than the mechanism we have studied, may have compensate for the asymmetries induced in our experiments during metaphase. In addition our analysis of later stages may have been biased by selecting for cells that were able to proceed into telophase. Dynein attachment caused a delay in mitosis (Figure 7A) and failure of cytokinesis (Figure 7C). Thus the asymmetries we observed late in mitosis are a potentially an underestimate of the consequences of failure to undergo motor shedding.

Mitotic arrest was one of the most pronounced consequences of attaching dynein to mitochondria and thereby linking them to the mitotic spindle (Figure 7C). This arrest was not observed with kinesin recruitment and thus correlates with spindle localization rather than general microtubule association or asymmetric distribution. Failure of cytokinesis also explains the prevalence of binucleate cells when dynein was recruited to the mitochondria.

We found that cytokinesis failure was due to steric interference of the bulky mitochondria with correct spindle function rather than depletion of endogenous free dynein required for other mitotic functions. Cytokinetic failure was not seen upon identical expression of the BICD construct when BICD was cytosolic in the absence of rapalog, but only when BICD was directed to mitochondria. Moreover, sequestering dynein to peroxisomes, a smaller organelle, did not produce equivalent failure of mitosis (Figure 7). The results with peroxisome recruitment are consistent with previous studies in which smaller organelles like early endosomes and fragmented Golgi vesicles attach to microtubules without defects to cytokinesis (Dunster et al., 2002; Jongsma et al., 2015). In contrast, ER recruitment to the spindle through a mechanism that should not have altered dynein availability, did produce binucleate cells (Figure 7). Thus the failure to exit mitosis correlates well with the presence of large organelles on the spindle that can interfere with chromosome segregation while smaller organelles pose no obstacle to mitotic fidelity.

These studies have identified a phosphorylation-driven mechanism that causes motor proteins to be shed from the mitochondrial surface in order to release mitochondria from microtubules. By selectively severing the association of mitochondria with microtubules at the time of spindle formation, mitochondria are permitted to take up a peripheral location during mitosis and subsequently undergo passive symmetric inheritance. Thus passive inheritance results from active regulation of the state of the motor/adaptor complex. Motor shedding has crucial consequences for the cell; it facilitates symmetrical distribution and inheritance of mitochondria while also clearing the spindle of an organelle that could arrest mitosis and prevent cytokinesis. Because the shedding releases the motors from the organelle but does not inhibit their microtubule interactions, kinesin and dynein remain free to serve their proper mitotic functions.

Experimental Procedures

Plasmid Constructs

For the sources of published plasmids and PCR-based construction of additional plasmids, see Extended Experimental Procedures.

Cell Culture and Transfection

HeLa, COS7, and HEK293T cells were cultured in DMEM containing L-glutamine, 10% FBS (Atlanta Premium), penicillin and streptomycin (Life Technologies). Rat embryonic fibroblasts were cultured in the same media with 20% FBS. Plasmid transfections were performed with Lipofectamine2000 (Life Technologies) 2 days prior to experiments.

Synchronization and Drug Treatments

Cells were treated with 2 mM thymidine for 16 h and released into fresh media for 8 hours followed by 16 h thymidine incubation. Fresh media was replaced for 8 hours for mitosis imaging, 10 hours for telophase, or 16 hours for G1. For biochemistry, cells were synchronized by treating with either 100 ng/mL nocodazole or 5 μM s-trityl-L-cysteine (STLC) for 16 hours instead of the second thymidine block. For actin experiments, cells

were treated for 10 minutes prior to fixation with 5 μm Latrunculin A or DMSO. For kinase inhibition, cells were treated with 10 μM RO-3306 or 2 mM ZM447439 for 16 hours.

Immunofluorescence and Protein Analysis

Cells were fixed for optimized microtubule stability: wash with PBS (phosphate buffered saline) and treat for 10 min with 3% paraformaldehyde, 0.1 M PIPES, 1 mM MgCl2, 100 mM EGTA, 0.05% saponin followed by a PBS wash and block with 3% bovine serum albumin (BSA), 0.1 M PIPES, 1 mM MgCl2, 100 mM EGTA, 0.05% saponin. Cells were stained with antibodies (see Extended Experimental Procedures) and imaged by confocal microscopy. Images were processed using ImageJ with linear adjustments to color and contrast. HeLa lysates were prepared similar to a previously used protocol (Glater et al., 2006). For immunoprecipitation and calf-intestinal phosphatase experiments see Extended Experimental Methods.

Statistical Analysis and Image Quantification

Statistical analysis was performed using GraphPad Prism v6.0e for MacOSX. Normality was determined using the D'Agostino & Pearson omnibus normality test. Student's t-test was used to determine the p value between the control and experimental conditions. For overlap calculations, the integrated density of fluorescence signals of mitochondria and tubulin were used to calculate the percent overlap. For mitochondrial overlap, the tubulin signal was thresholded by mean to create a mask to measure the overlapping mitochondrial signal, which was then divided by the total mitochondrial signal. For percent mitotic cells, 10 fields at 40x were captured at each time point, and the percent of mitotic cells was calculated and averaged. For the percent of binucleate cells, the average percentage of binucleate cells was calculated for 3 sets of 30 transfected cells. Scatter plots of asymmetric index for either metaphase or telophase are expressed as the median with bars extending to the first and third quartile. The Kolmogorov-Smirnov test was used to determine significance between the control and experimental conditions. $p < 0.05$ was considered significant.

Supplementary Material

Refer to Web version on PubMed Central for supplementary material.

Acknowledgments

We thank Drs. G. Hajnóczky; C. Hoogenraad; K.J. Verhey; K.K. Pfister; E.L. Holzbaur; T. Rapoport; D. Kashatus; A. Akhmanova; G. Banker; and T. Inoue for reagents. We thank L. Ding and D. Tom from Harvard NeuroDiscovery Center, Enhanced Neuroimaging Core, T. Hill from the Cellular Imaging Core at Boston Children's Hospital for imaging assistance, and J.F.K. Sauld, S. Ahmed, H. Chen from the Proteomics Center at Boston Children's Hospital for mass spectroscopy assistance. This work was supported by F31GM108199-03 (JYC), 2R01GM069808 (TLS), the Mathers Foundation (TLS) and the IDDRC Molecular Genetics, Proteomics, and Imaging Cores (P30HD18655).

References

Allan VJ, Vale RD. Cell cycle control of microtubule-based membrane transport and tubule formation in vitro. The Journal of cell biology. 1991; 113:347–359. [PubMed: 2010466]

Baggethun P. 2009 Radial Profile Plot (http://rsb.info.nih.gov/ij/plugins/radial-profile.html: U. S. National Institutes of Health, Bethesda, Maryland, USA).

Ball EH, Singer SJ. Mitochondria are associated with microtubules and not with intermediate filaments in cultured fibroblasts. Proceedings of the National Academy of Sciences of the United States of America. 1982; 79:123–126. [PubMed: 6275382]

de Brito OM, Scorrano L. Mitofusin 2 tethers endoplasmic reticulum to mitochondria. Nature. 2008; 456:605–610. [PubMed: 19052620]

Dell KR, Turck CW, Vale RD. Mitotic phosphorylation of the dynein light intermediate chain is mediated by cdc2 kinase. Traffic (Copenhagen, Denmark). 2000; 1:38–44.

Dunster K, Toh BH, Sentry JW. Early endosomes, late endosomes, and lysosomes display distinct partitioning strategies of inheritance with similarities to Golgi-derived membranes. European journal of cell biology. 2002; 81:117–124. [PubMed: 11998863]

Fransson S, Ruusala A, Aspenstrom P. The atypical Rho GTPases Miro-1 and Miro-2 have essential roles in mitochondrial trafficking. Biochem Biophys Res Commun. 2006; 344:500–510. [PubMed: 16630562]

Glater EE, Megeath LJ, Stowers RS, Schwarz TL. Axonal transport of mitochondria requires milton to recruit kinesin heavy chain and is light chain independent. The Journal of cell biology. 2006; 173:545–557. [PubMed: 16717129]

Guo X, Macleod GT, Wellington A, Hu F, Panchumarthi S, Schoenfield M, Marin L, Charlton MP, Atwood HL, Zinsmaier KE. The GTPase dMiro is required for axonal transport of mitochondria to Drosophila synapses. Neuron. 2005; 47:379–393. [PubMed: 16055062]

Hoogenraad CC, Wulf P, Schiefermeier N, Stepanova T, Galjart N, Small JV, Grosveld F, de Zeeuw CI, Akhmanova A. Bicaudal D induces selective dynein-mediated microtubule minus end-directed transport. The EMBO journal. 2003; 22:6004–6015. [PubMed: 14609947]

Jongsma ML, Berlin I, Neefjes J. On the move: organelle dynamics during mitosis. Trends Cell Biol. 2015; 25:112–124. [PubMed: 25466831]

Kanfer G, Courtheoux T, Peterka M, Meier S, Soste M, Melnik A, Reis K, Aspenstrom P, Peter M, Picotti P, et al. Mitotic redistribution of the mitochondrial network by Miro and Cenp-F. Nat Commun. 2015; 6:8015. [PubMed: 26259702]

Kashatus D, Lim K-H, Brady D, Pershing N, Cox A, Counter C. RALA and RALBP1 regulate mitochondrial fission at mitosis. Nature cell biology. 2011; 13:1108–1115. [PubMed: 21822277]

Katajisto P, Dohla J, Chaffer C, Pentinmikko N, Marjanovic N, Iqbal S, Zoncu R, Chen W, Weinberg RA, Sabatini DM. Asymmetric apportioning of aged mitochondria between daughter cells is required for stemness. Science (New York, NY). 2015

Lawrence E, Mandato C. Mitochondrial inheritance is mediated by microtubules in mammalian cell division. Commun Integr Biol. 2013a; 6:e27557. [PubMed: 24567781]

Lawrence EJ, Boucher E, Mandato CA. Mitochondria-cytoskeleton associations in mammalian cytokinesis. Cell Div. 2016; 11:3. [PubMed: 27030796]

Lawrence EJ, Mandato CA. Mitochondria localize to the cleavage furrow in mammalian cytokinesis. PloS one. 2013c; 8:e72886. [PubMed: 23991162]

Lee S, Kim S, Sun X, Lee J-H, Cho H. Cell cycle-dependent mitochondrial biogenesis and dynamics in mammalian cells. Biochemical and biophysical research communications. 2007; 357:111–117. [PubMed: 17400185]

Martinez-Diez M, Santamaria G, Ortega AD, Cuezva JM. Biogenesis and dynamics of mitochondria during the cell cycle: significance of 3'UTRs. PloS one. 2006; 1:e107. [PubMed: 17205111]

Mishra P, Chan DC. Mitochondrial dynamics and inheritance during cell division, development and disease. Nat Rev Mol Cell Biol. 2014; 15:634–646. [PubMed: 25237825]

Niclas J, Allan VJ, Vale RD. Cell cycle regulation of dynein association with membranes modulates microtubule-based organelle transport. The Journal of cell biology. 1996; 133:585–593. [PubMed: 8636233]

Olsen J, Vermeulen M, Santamaria A, Kumar C, Miller M, Jensen L, Gnad F, Cox J, Jensen T, Nigg E, et al. Quantitative phosphoproteomics reveals widespread full phosphorylation site occupancy during mitosis. Science signaling. 2010:3.

Park YY, Cho H. Mitofusin 1 is degraded at G2/M phase through ubiquitylation by MARCH5. Cell Div. 2012; 7:25. [PubMed: 23253261]

Pathak D, Sepp KJ, Hollenbeck PJ. Evidence that myosin activity opposes microtubule-based axonal transport of mitochondria. J Neurosci. 2010; 30:8984–8992. [PubMed: 20592219]

Raaijmakers JA, Tanenbaum ME, Medema RH. Systematic dissection of dynein regulators in mitosis. The Journal of cell biology. 2013; 201:201–215. [PubMed: 23589491]

Rohn JL, Patel JV, Neumann B, Bulkescher J, McHedlishvili N, McMullan RC, Quintero OA, Ellenberg J, Baum B. Myo19 ensures symmetric partitioning of mitochondria and coupling of mitochondrial segregation to cell division. Current biology : CB. 2014; 24:2598–2605. [PubMed: 25447992]

Smyth JT, Beg AM, Wu S, Putney JW Jr, Rusan NM. Phosphoregulation of STIM1 Leads to Exclusion of the Endoplasmic Reticulum from the Mitotic Spindle. Current biology : CB. 2012; 22:1487–1493. [PubMed: 22748319]

Stowers RS, Megeath LJ, Gorska-Andrzejak J, Meinertzhagen IA, Schwarz TL. Axonal transport of mitochondria to synapses depends on milton, a novel Drosophila protein. Neuron. 2002; 36:1063–1077. [PubMed: 12495622]

Symens N, Soenen SJ, Rejman J, Braeckmans K, De Smedt SC, Remaut K. Intracellular partitioning of cell organelles and extraneous nanoparticles during mitosis. Advanced drug delivery reviews. 2012; 64:78–94. [PubMed: 22210278]

van Spronsen M, Mikhaylova M, Lipka J, Schlager MA, van den Heuvel DJ, Kuijpers M, Wulf PS, Keijzer N, Demmers J, Kapitein LC, et al. TRAK/Milton motor-adaptor proteins steer mitochondrial trafficking to axons and dendrites. Neuron. 2013; 77:485–502. [PubMed: 23395375]

Westermann B. Mitochondrial inheritance in yeast. Biochimica et biophysica acta. 2014; 1837:1039–1046. [PubMed: 24183694]

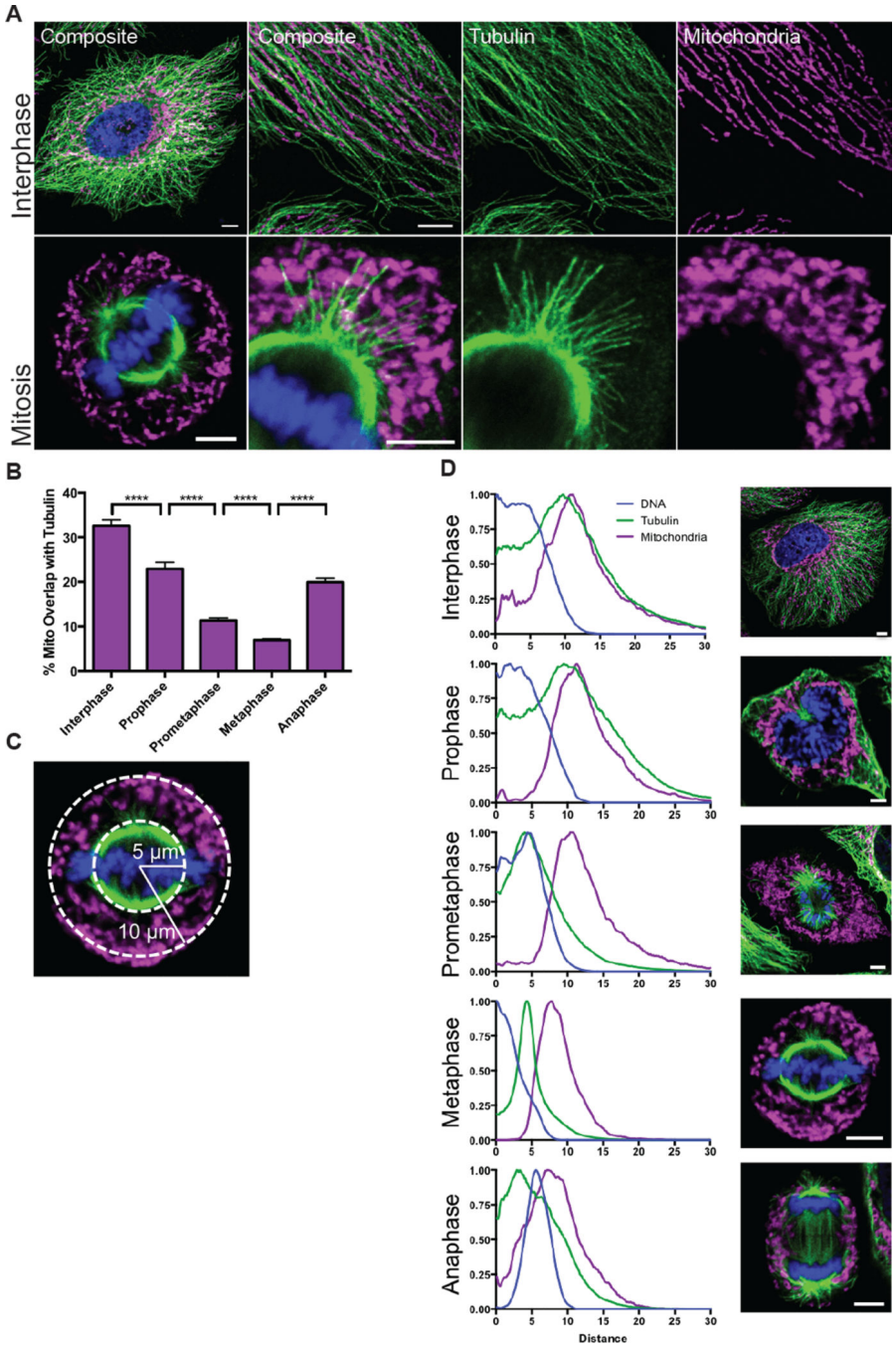

Figure 1. Mitochondria are released from microtubules during cell division

(A) Interphase and mitotic HeLa cells were stained for TOM20 (magenta), a mitochondrial marker, tubulin (green), and DNA (Hoechst 33342, blue) and imaged by confocal microscopy at 63x and 100x. (B) Percent of the total mitochondrial area that overlapped with tubulin during each mitotic phase. (C) Schematic of how the radial distributions of tubulin and mitochondria were calculated relative to the center of the DNA. (D) The radial distributions were averaged for 30 cells for each mitotic phase. Images are representative of

the phase. ****$p < 0.0001$; All values are shown as mean ± SEM. Scale bars represent 5 microns.

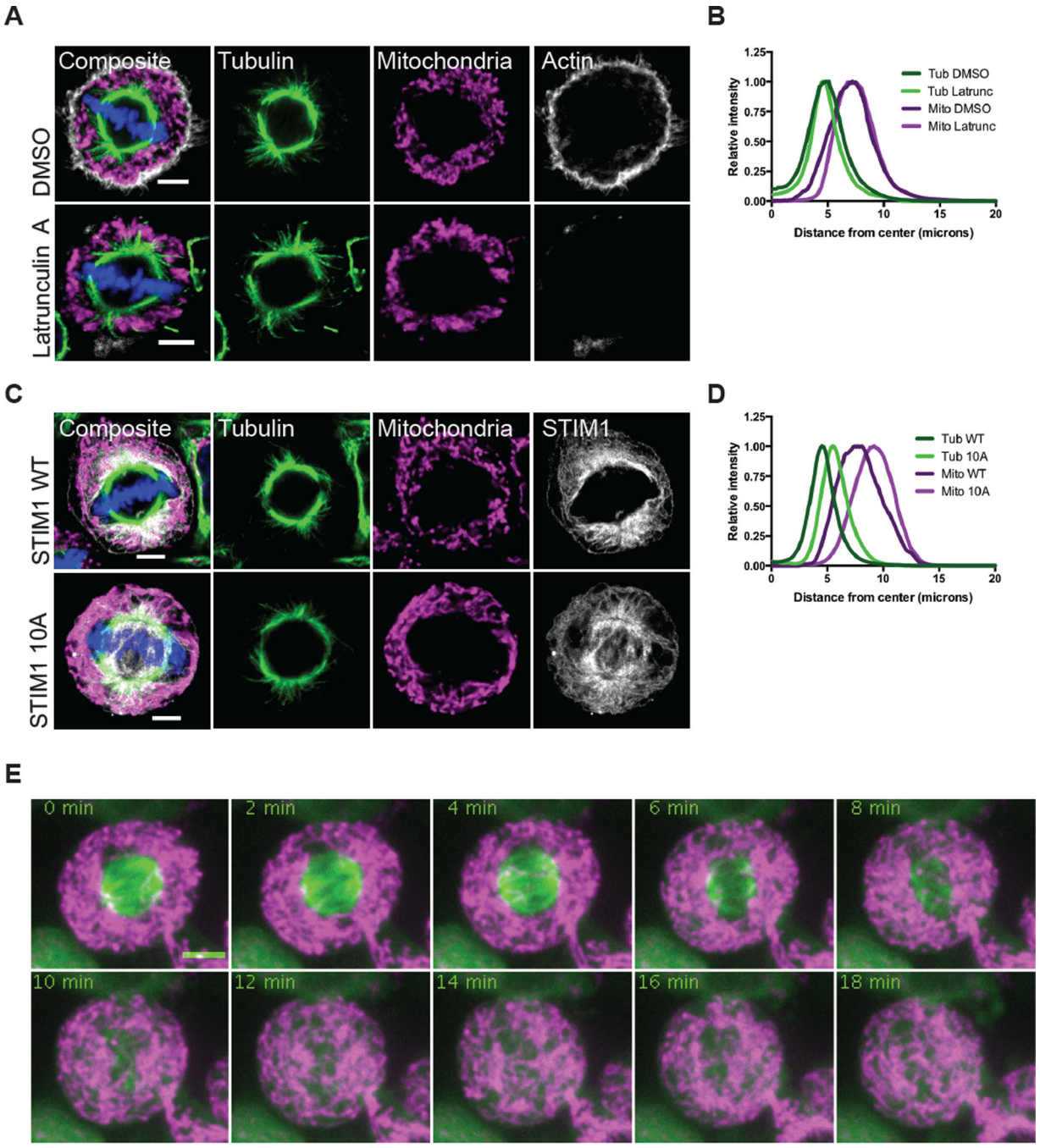

Figure 2. Mitochondrial distribution is independent of actin or ER tethering during mitosis

(A) HeLa cells were synchronized into metaphase cells and treated for 10 min with DMSO or Latrunculin A prior to fixation. Mitochondria (TOM20, magenta), tubulin (green), and actin filaments (grey) were immunostained and imaged by confocal microscopy. (B) The radial distributions of tubulin and mitochondria were averaged for 30 metaphase cells treated as in (A). (C) HeLa cells were transiently transfected with STIM1 constructs. Mitochondria (TOM20, magenta), tubulin (green), and STIM1 (grey) were immunostained and imaged by confocal microscopy. (D) The radial distributions of tubulin and mitochondria were averaged

for 30 metaphase cells expressing STIM1 WT or STIM 10A as in (C). (E) HeLa cells were transfected with Mito-dsRed and GFP-tubulin and synchronized. Cells were treated with nocodazole (0 min) and images were taken every 2 minutes. Scale bars represent 5 microns.

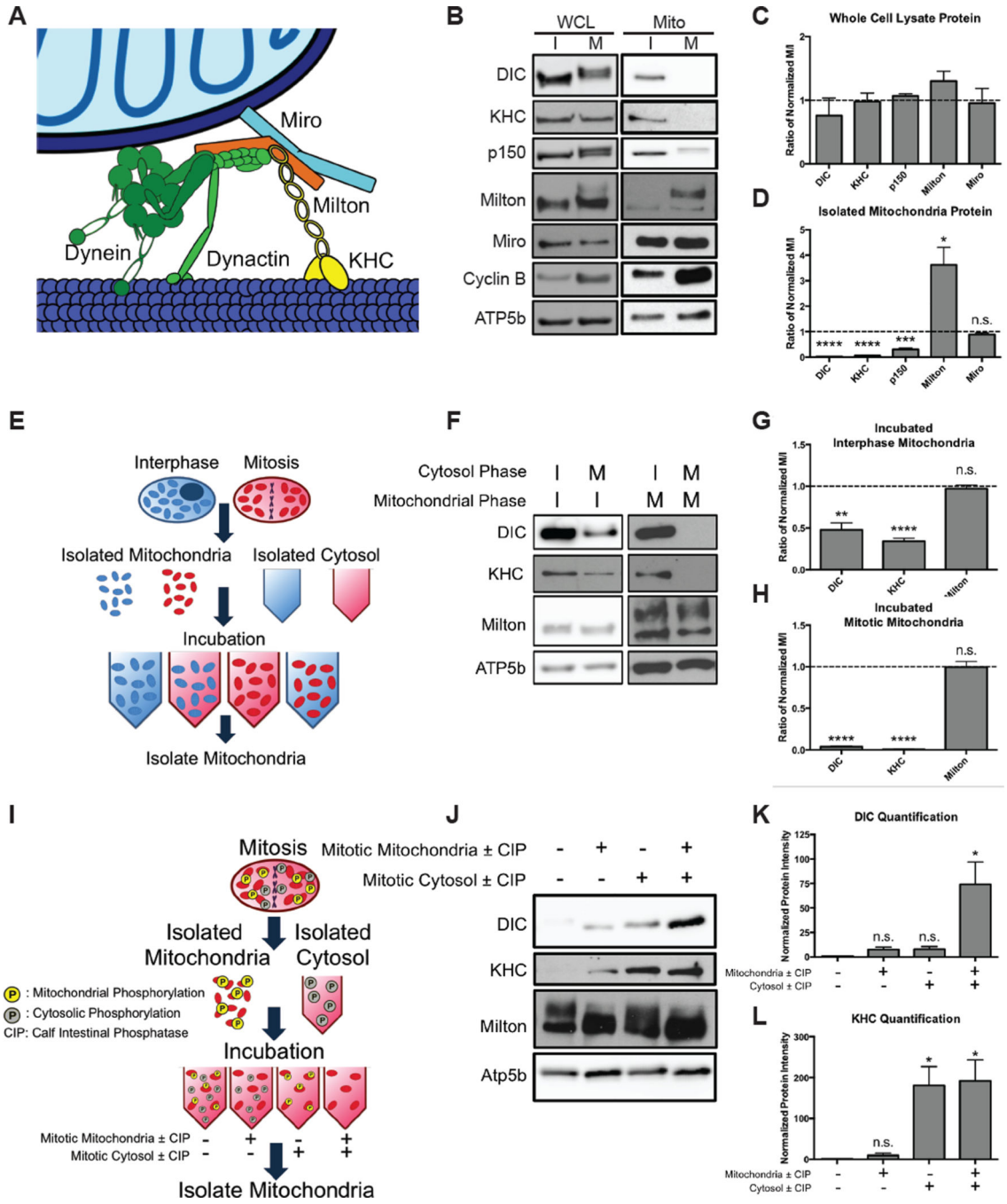

Figure 3. Phosphorylation detaches dynein and kinesin motors from mitochondria during mitosis

(A) Schematic of the motor adaptor complex including Miro, Milton, kinesin (KHC), dynein and dynactin. (B–D) HeLa cells were synchronized into interphase or mitosis (nocodazole-induced arrest). Whole cell lysates (WCL) and isolated mitochondria (Mito) were probed for the indicated proteins of the motor adaptor complex. Levels of the motor protein subunits were reduced on mitotic mitochondria, but Milton and Miro remained on mitochondria. Several protein's positions were altered by mitotic phosphorylations. Elevated Cyclin B levels verified that cells were in mitosis, and the mitochondrial protein ATP5b verified equal

mitochondrial content in the samples. Band intensities were quantified (C,D), and each mitotic protein was normalized to the level of that protein at interphase and the fold changes are shown. n = 3. (E–H) Schematic, immunoblot, and quantification of a biochemical assay to determine if interphase or mitotic cytosol can alter the mitochondrial association of the motors. Mitochondria from either interphase (I) or mitosis (M) were incubated with interphase or mitotic cytosol. Mitochondria were re-isolated and assayed for the indicated proteins. Mitotic cytosol induced motor release, and interphase cytosol reattached motors in the assay. Band intensities were quantified, and the relative effects of the two types of cytosol were compared by normalizing the intensity of the band with mitotic cytosol to that with interphase cytosol. The fold changes for interphase mitochondria (G) and mitotic mitochondria (H) so treated are shown. n = 3. (I–L) Assay to determine if treatment with calf intestinal phosphatase (CIP) can allow motors to reattach. The mitochondrial and cytosolic fractions were treated with either CIP alone (+) or CIP and the phosphatase inhibitor NaVO4 (−) prior to being recombined. Mitochondria were re-isolated and probed for the indicated proteins. DIC (K) and KHC (L) levels were quantified and normalized to the untreated fraction condition. n = 3. *p < 0.05, **p < 0.01, ***p < 0.001, ****p < 0.0001.

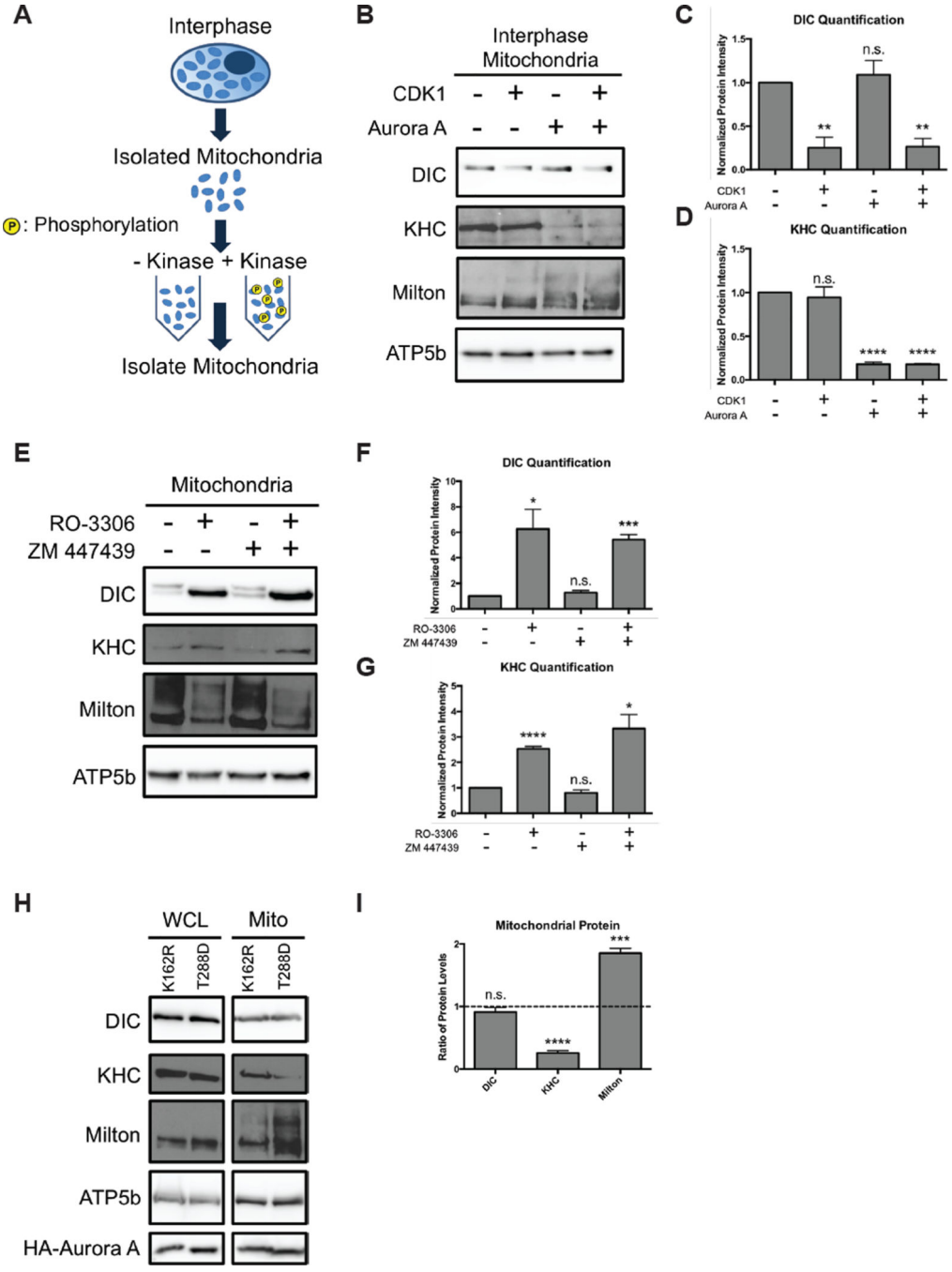

Figure 4. CDK1 and Aurora A induce motor release

(A–D) Schematic, immunoblot, and quantification of proteins on interphase mitochondria treated with or without active, purified CDK1 and Aurora A as indicated. Dynein and kinesin band intensities were quantified and normalized to the untreated fraction condition. n = 3. (E–G) Mitotic HeLa cells were treated with the CDK1 inhibitor RO-3306 and/or the Aurora inhibitor ZM447439. Isolated mitochondria were probed for the indicated proteins. Levels of DIC and KHC were quantified and normalized to the untreated fraction condition. n = 3. (H,I) HeLa cells were transfected with inactive (K162R) or constitutively active

(T288D) Aurora A kinase. Whole cell extracts (WCL) and mitochondria (Mito) were probed for the indicated proteins. Protein levels were quantified, normalized to the loading control, and then expressed as the ratio of the level in the T288D cells to K162R cells. n = 3. *p < 0.05, **p < 0.01, ***p < 0.001, ****p < 0.0001.

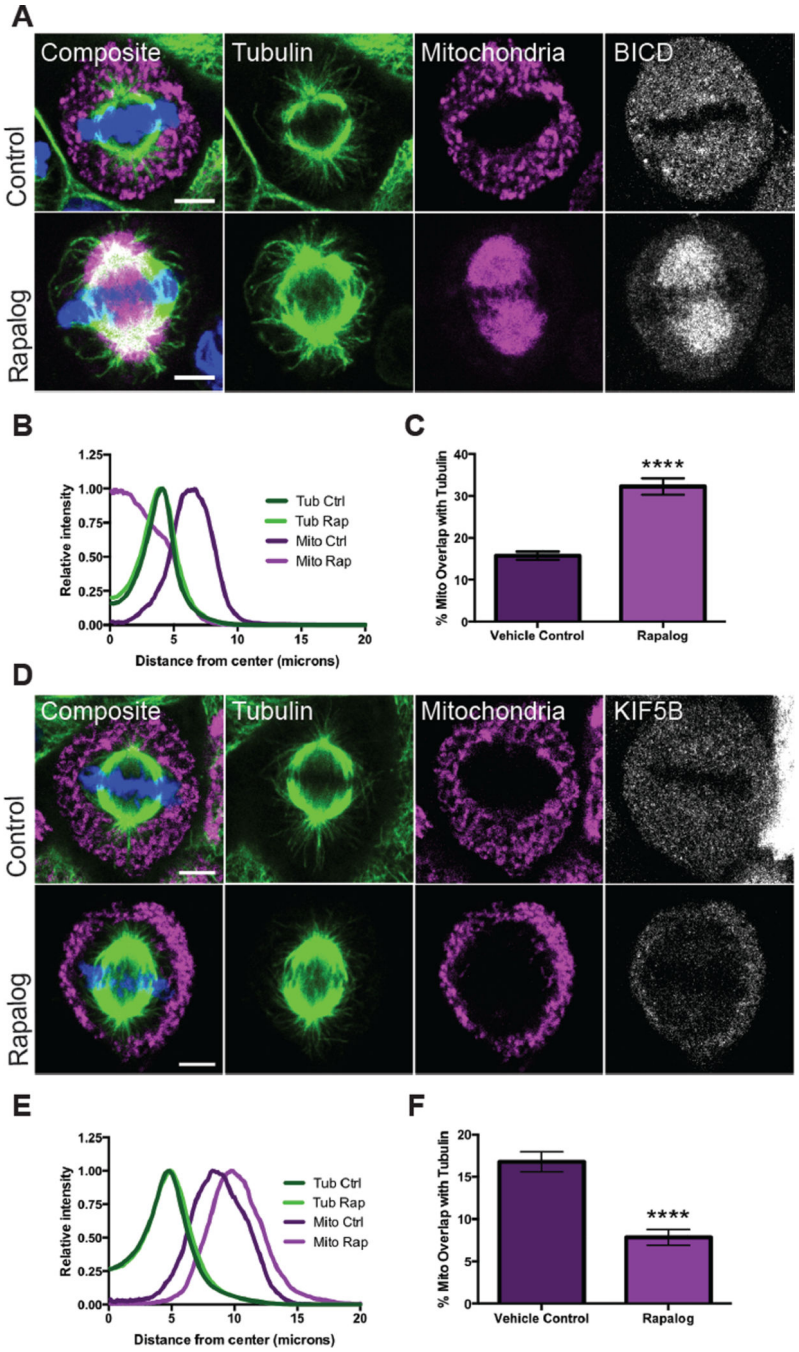

Figure 5. Coupling motors to mitochondria during cell division mislocalizes the mitochondria

(A–C) HeLa cells transiently expressing Tom20-mCherry-FKBP and the dynein-binding construct HA-BICD2-FRB were synchronized and treated with ethanol (control) or the heterodimizer rapalog 10 minutes prior to fixation. Rapalog addition forced mitochondria onto the spindle. Averaged radial distribution (B) and percent overlap of mitochondrial and tubulin signals (C) for 30 cells in each condition. (D–F) HeLa cells transiently expressing Tom20-mCherry-FKBP and HA-KIF5B MD-FRB were synchronized and treated with ethanol (control) or rapalog for 10 minutes prior to fixation. Rapalog caused mitochondria to

assume a more peripheral localization. Averaged radial distribution (E) and percent overlap of mitochondrial and tubulin signals (F) for 30 cells in each condition. Data are represented as mean ± SEM. Scale bars represent 5 microns. **** p <0.0001

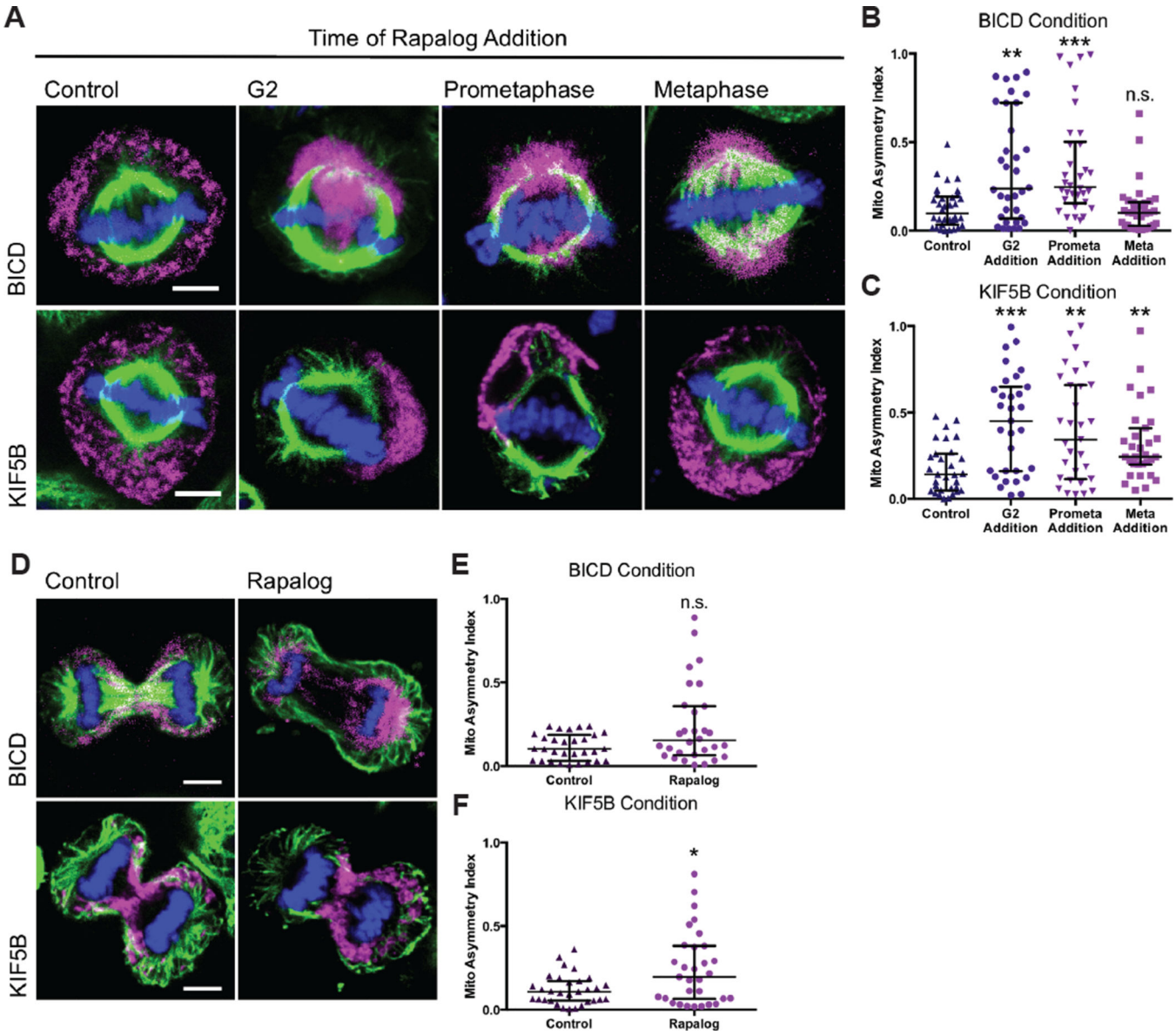

Figure 6. Coupling motors to mitochondria during cell division causes mitochondrial asymmetry

(A–C) HeLa cells transiently expressing Tom20-mCherry-FKBP and either HA-BICD2-FRB or HA-KIF5B MD-FRB were treated with ethanol (control) or rapalog at G2, prometaphase, or metaphase and imaged by confocal microscopy at metaphase. The asymmetric index of metaphase cells was calculated on 3D projections of treated cells for BICD-FRB transfected cells (B) and KIF5B–FRB transfected cells (C). (D–F) HeLa cells transfected as in (A) were imaged during telophase. An asymmetric index of the two daughters cells mitochondrial content was calculated for cells expressing BICD-FRB (E) or KIF5B–FRB (F). Data are represented as median with the interquartile range. Scale bars represent 5 microns. *$p < 0.05$, **$p < 0.01$, ***$p < 0.001$.

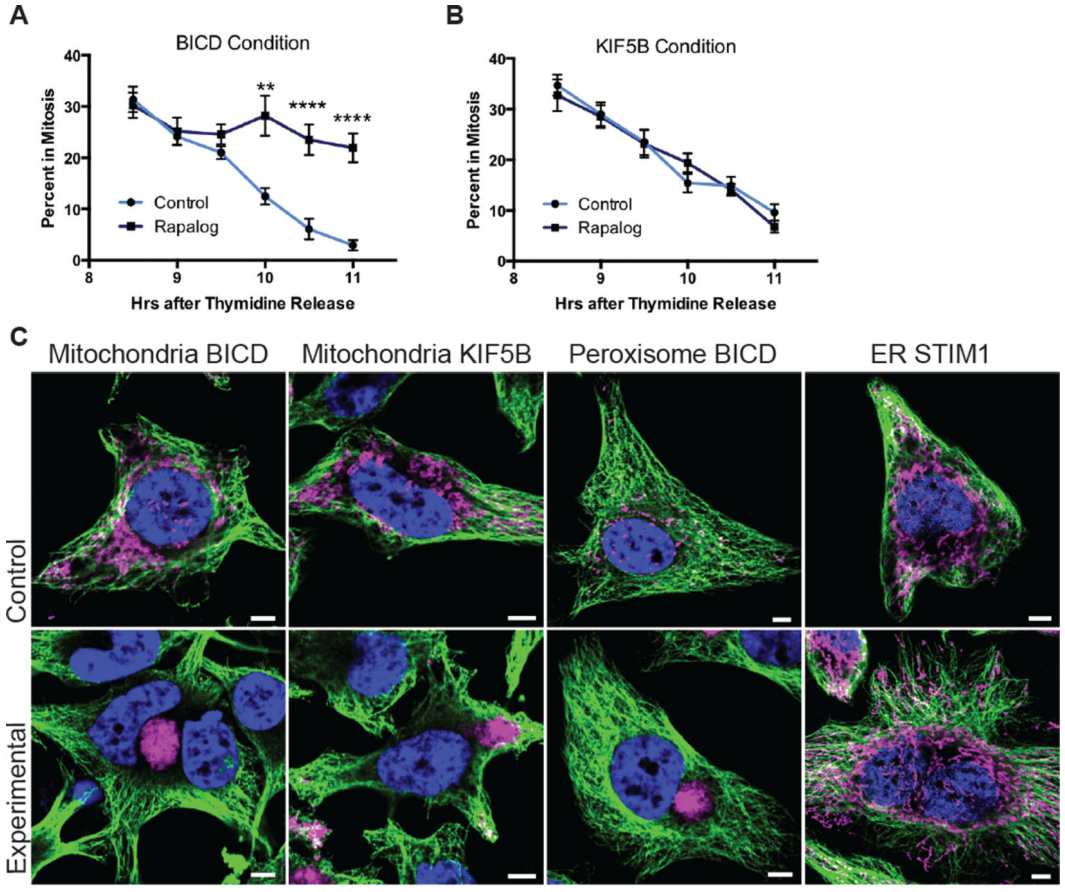

E

Number of Binucleated Cells

Out of 90 cells	Mito-BICD	Mito-KIF5B	PEX-BICD	STIM1
Control	3	8	5	2
Experimental	48	10	8	14

Figure 7. Organelle attachment to spindle microtubules causes mitotic arrest and binucleate cells

HeLa cells transiently expressing Tom20-mCherry-FKBP and either HA-BICD2-FRB (A) or HA-KIF5B MD-FRB (B) were released from thymidine block and treated with ethanol (control) or rapalog. The percentage of transfected cells in mitosis was determined at the indicated times after thymidine block release. Vehicle treated cells and those expressing KIF5B-FRB proceeded normally through mitosis, but rapalog-treated BICD-FRB expressing cells failed to exit mitosis. (C–E) HeLa cells were transiently transfected with the following constructs: Tom20-mCherry-FKBP and HA-BICD-FRB (Mitochondria BICD); Tom20-

mCherry-FKBP and HA-KIF5B MD-FRB (Mitochondria KIF5B); PEX-RFP-FKBP and HA-BICD-FRB (Peroxisome BICD); STIM1 WT (ER STIM1, control) or STIM1 10A (ER STIM1, experimental). The cells with FKBP and FRB constructs were treated with either ethanol (control) or rapalog (experimental) during G2. (C) Tubulin (green), DNA (blue) and mCherry/Tom20 (mitochondria, magenta) or RFP (peroxisomes, magenta) were imaged by confocal microscopy. (D) The percentages of binucleate cells from three independent experiments were averaged and compared by Student's t-test. A table of the actual cell counts are shown in (E). Scale bars represent 5 microns. Data are represented as mean ± SEM. *$p < 0.05$, **$p < 0.01$, ***$p < 0.001$.